Third-order differential ladder operators and supersymmetric quantum mechanics

2008 J. Phys. A: Math. Theor. 41 045204

(http://iopscience.iop.org/1751-8121/41/4/045204)

IOP PUBLISHING JOURNAL OF PHYSICS A: MATHEMATICAL AND THEORETICAL

J. Phys. A: Math. Theor. **41** (2008) 045204 (28pp) doi:10.1088/1751-8113/41/4/045204

Third-order differential ladder operators and supersymmetric quantum mechanics

J Mateo and J Negro

Departamento de Física Teórica, Atómica y Óptica, Facultad de Ciencias, E-47011 Valladolid, Spain

E-mail: jmateo@metodos.fam.cie.uva.es

Received 28 June 2007, in final form 16 November 2007
Published 15 January 2008
Online at stacks.iop.org/JPhysA/41/045204

Abstract

Hierarchies of one-dimensional Hamiltonians in quantum mechanics admitting third-order differential ladder operators are studied. Each Hamiltonian has associated three-step Darboux (pseudo)-cycles and Painlevé IV equations as a closure condition. The whole hierarchy is generated applying some operations on the cycles. These operations are investigated in the frame of supersymmetric quantum mechanics and mainly involve algebraic manipulations. A consistent geometric representation for the hierarchy and cycles is built that also helps in understanding the operations. Three kinds of hierarchies are distinguished and a realization based on the harmonic oscillator Hamiltonian is supplied, giving an interpretation for the spectral properties of the Hamiltonians of each hierarchy.

PACS numbers: 02.30.Hq, 03.65.Ge

(Some figures in this article are in colour only in the electronic version)

1. Introduction

The aim of this work is finding Hamiltonians of the Schrödinger form

$$H = -\frac{\mathrm{d}^2}{\mathrm{d}x^2} + V(x), \tag{1}$$

which admit a third-order differential ladder operator (DLO) of the kind of shift operators, i.e., with a linear spectrum, using supersymmetric quantum mechanics (SUSY-QM) techniques [1, 2].

The third-order operator $\mathcal{L}$ will be a DLO of the Hamiltonian H if the following commutation relation holds

$$[H, \mathcal{L}] = \gamma\mathcal{L} \quad \Longleftrightarrow \quad \mathcal{L}H = (H - \gamma)\mathcal{L}. \tag{2}$$

The last expression has the form of the standard SUSY intertwining relation [3]

$$L H_1 = H_2 L, \tag{3}$$

where L is an intertwining differential operator, and the Hamiltonians H_1, H_2 are said to be SUSY partners. Sometimes L is referred also as a SUSY or Darboux transformation and usually it is of first order; when L is of third order an italic style $\mathcal{L}$ is used. If the partner potential H_2 is the original one but shifted $(H_1 - \gamma)$ the ladder commutation relation (2) is recovered from (3).

The factorization of the third-order SUSY transformation $\mathcal{L}$ in equation (2) as a three-step chain of 1-SUSY transformations [4] gives a (pseudo) cyclic chain. The closure condition for the cycle leads precisely to a P_{IV} equation [4–8]. Furthermore, as the factorization of $\mathcal{L}$ is not unique, the consecutive modifications on the cycle lead to different P_{IV} equations enabling the construction of hierarchies of Hamiltonians with third-order ladder operators and to transformation properties between solutions of P_{IV} equations with different parameters. Other approaches dealing with different aspects of P_{IV} hierarchies have been considered in the literature [9–11].

This work is organized as follows. In the second section, we review the main properties of 1-SUSY transformations. The three-step chain transformation, the introduction of intermediate Hamiltonians and a P_{IV} equation as the condition that enables (2) to be fulfilled will be the subject of section 3. The following section will deal with the construction of hierarchies: basic operations to find new Hamiltonians with DLO's or to generate new solutions of the corresponding P_{IV} equation, and a consistent geometrical representation for any hierarchy. We will also find a fundamental cell for the parameters of independent P_{IV} hierarchies. In sections 5–8, the harmonic oscillator is presented as the Hamiltonian from which known P_{IV} solutions can be derived. Three kinds of hierarchies are given and using the geometrical representation it is shown how the spectral properties of Hamiltonians are modified and how the regular P_{IV} solutions are distributed. In the final section (section 9) we will add some conclusions and remarks.

2. 1-SUSY transformations

When the intertwining operator (IO) in (3) is a first-order differential operator L is called 1-SUSY transformation; its explicit form is [3, 12–15]

$$L := \partial_x - f(x), \tag{4}$$

where $f(x)$ is a function called superpotential defined as

$$f(x) := \frac{u'(x)}{u(x)}. \tag{5}$$

The generating function $u(x)$ is an eigenfunction of H_1, not necessary square-integrable, and constitutes the kernel of L. Let λ be the associated eigenvalue, $H_1 u(x) = \lambda u(x)$, called factorization eigenvalue then, potential $V_1(x)$ (1) of H_1 can be written as

$$V_1(x) = f'(x) + f(x)^2 + \lambda, \tag{6}$$

and the SUSY partner H_2 has the related potential

$$V_2 = V_1 - 2f'(x). \tag{7}$$

From (3) it follows that L transforms eigenfunctions of H_1 into eigenfunctions of H_2 with the same eigenvalue. We consider the eigenfunctions in a wide sense and we will call them 'physical' if they are square-integrable with appropriate boundary conditions.

In order to obtain partner potentials $V_2(x)$ without new singularities, we see from (7) that the generating eigenfunctions $u(x)$ must have no vanishing points. Two kind of eigenfunctions have usually been used in this respect [3, 12–14]: (i) the ground-state wavefunction of H_1. In this case, the spectrum corresponding to physical eigenfunctions of H_2 is the same as H_1, except for the ground energy that is missing. (ii) Non-vanishing eigenfunctions with λ below the ground-state energy. In this case, the spectrum of H_2 is either identical to H_1 or includes the new point λ.

The eigenfunctions with eigenvalues above the ground level have vanishing points, thus leading to singular potentials. However, these singularities can be removed through another SUSY transformation using an eigenfunction with intercalated vanishing points with the initial one, then the resulting 2-SUSY partner potential is regular [16].

In this paper, we are interested in a general application of SUSY transformations and we will keep in mind the possibility of using any eigenfunction even if the potential or superpotential have additional singularities.

It is possible to find an intertwining relation in the opposite direction of relation (3)

$$H_1 L^+ = L^+ H_2 \tag{8}$$

defining the differential operator

$$L^+ := -\partial_x - f(x). \tag{9}$$

Therefore, L^+ takes eigenfunctions of H_2 into eigenfunctions of H_1:

$$H_1 \underset{L^+,\lambda}{\overset{L,\lambda}{\rightleftarrows}} H_2 \tag{10}$$

leading to the factorization of both SUSY Hamiltonians

$$H_1 = L^+ L + \lambda \qquad H_2 = L L^+ + \lambda, \tag{11}$$

where λ is the factorization eigenvalue of the generating eigenfunction $u(x)$. It is worth noting that in the literature L^+ is identified with the adjoint of L but it is only true for $f(x)$ real, i.e., the Hermitian case. When $f(x)$ is complex the operator defined in (9) is no longer the adjoint but the reverse operation is still accomplished by it. However, the partner Hamiltonian will be complex [17].

3. 3-SUSY transformations and P_{IV} equations

Chains of SUSY transformations have been widely studied [5–8, 18], here we will consider a 3-SUSY (pseudo)-cyclic transformation that can be written as a three-step chain of 1-SUSY transformations. Let H_1 be a Hamiltonian (1) and $\mathcal{L}$ a third-order differential ladder operator, it can be factorized as [18–20]

$$\mathcal{L} = L_3 L_2 L_1 = (\partial_x - f_3)(\partial_x - f_2)(\partial_x - f_1) \tag{12}$$

such that each factor is a 1-SUSY transformation

$$H_i \xrightarrow{L_i} H_{i+1} \tag{13}$$

$$H_i u_i = \alpha_i u_i, \qquad L_i = \partial_x - f_i, \qquad f_i = \frac{u_{ix}}{u_i} \qquad i \in \{1, 2, 3\}, \tag{14}$$

where H_4 is the shifted original Hamiltonian. In the most general case superpotentials and intermediate potentials can be complex, but for simplicity we will assume henceforth that

these factors are real in order to obtain Hermitian intermediate Hamiltonians, although they can present singularities, leading to a dressing chain of Hamiltonians [8]. Therefore, the following representations are equivalent[1]:

$$\begin{array}{ccccccc} H_1 & & \xrightarrow{\qquad\qquad\mathcal{L}\qquad\qquad} & & & & H_1-2 \\ & & \Updownarrow & & & & \\ H_1 & \xrightarrow[L_1,\alpha_1]{} & H_2 & \xrightarrow[L_2,\alpha_2]{} & H_3 & \xrightarrow[L_3,\alpha_3]{} & H_1-2 \end{array} \tag{15}$$

where H_2 and H_3 are auxiliary partner Hamiltonians.

3.1. Factorization properties of $\mathcal{L}$

Let $\mathcal{K}$ be the kernel of $\mathcal{L}$, i.e. $\psi \in \mathcal{K} \Leftrightarrow \mathcal{L}\psi = 0$, then as $\mathcal{L}$ is a third-order differential operator $\mathcal{K}$ has dimension three. From (2) it is straightforward to see that $\mathcal{K}$ is invariant under H_1. Therefore, by a convenient choice of the basis of $\mathcal{K}$ we can express H_1, restricted to $\mathcal{K}$ in the standard Jordan matrix form with the following possibilities:

(i) *Hyperconfluent*. The Hamiltonian has one eigenvalue in $\mathcal{K}$. As H_1 is a second-order differential operator then it is not possible to find three independent eigenfunctions corresponding to this value. Thus, we have two options for the Jordan matrix,

$$\text{(a)} \quad \begin{pmatrix} \lambda_1 & \cdot & \cdot \\ 1 & \lambda_1 & \cdot \\ \cdot & 1 & \lambda_1 \end{pmatrix}; \qquad \text{(b)} \quad \begin{pmatrix} \lambda_1 & \cdot & \cdot \\ \cdot & \lambda_1 & \cdot \\ \cdot & 1 & \lambda_1 \end{pmatrix}. \tag{16}$$

In the case (b) the kernel includes two independent eigenfunctions of H_1 which means that $\mathcal{L}$ must take the form $\mathcal{L} = L_3(H_1 - \lambda_1)$. Then we will say that $\mathcal{L}$ is reducible. In this case, the cycle would include two identical Hamiltonians:

$$H_1 \xrightarrow[L_1,\lambda_1]{} H_2 \xrightarrow[L_2,\lambda_1]{} H_1 \xrightarrow[L_3,\lambda_1]{} H_1 - 2 \tag{17}$$

This situation is only possible when H_1 is the harmonic oscillator Hamiltonian.

(ii) *Confluent.* The Hamiltonian has two eigenvalues in $\mathcal{K}$. We also have two options for the Jordan matrix representation:

$$\text{(a)} \quad \begin{pmatrix} \lambda_1 & \cdot & \cdot \\ \cdot & \lambda_2 & \cdot \\ \cdot & \cdot & \lambda_2 \end{pmatrix}; \qquad \text{(b)} \quad \begin{pmatrix} \lambda_1 & \cdot & \cdot \\ \cdot & \lambda_2 & \cdot \\ \cdot & 1 & \lambda_2 \end{pmatrix}. \tag{18}$$

In the case (a) the same considerations of the hyperconfluent case (1.b) above apply, therefore $\mathcal{L}$ is reducible and H_1 must also be the harmonic oscillator. It is possible to find a basis made of eigenfunctions of H_1.

(iii) *Non-degenerated.* Now the Hamiltonian has three different eigenvalues. The Jordan matrix is diagonal

$$\begin{pmatrix} \lambda_1 & \cdot & \cdot \\ \cdot & \lambda_2 & \cdot \\ \cdot & \cdot & \lambda_3 \end{pmatrix} \tag{19}$$

then, $\mathcal{K}$ admits a basis made of Hamiltonian eigenfunctions.

[1] From now on the shift constant γ in (2) will be fixed to 2. This can always be done through a rescaling of the variable x and the potential. Some expressions will be simplified and the P_{IV} equation will be obtained in the standard form.

This classification is related to the different Hamiltonian hierarchies that will be shown in sections 6–8.

Let $\mathcal{L}^+ = L_1^+ L_2^+ L_3^+$, then $[H_1, \mathcal{L}^+] = -2\mathcal{L}^+$, and $\mathcal{L}^+$ is a lowering operator. Another useful property comes from the fact that since the operators $\mathcal{L}^+\mathcal{L}$ and $\mathcal{L}\mathcal{L}^+$ commute with the Hamiltonian H_1, they must be functions of H_1 [4, 8, 21, 22]:

$$\mathcal{L}^+\mathcal{L} = f(H_1), \qquad \mathcal{L}\mathcal{L}^+ = g(H_1). \tag{20}$$

The functions $f(H_1), g(H_1)$ must be third-order polynomials. The factorization of each polynomial depends on the eigenvalues of the eigenfunctions annihilated by $\mathcal{L}^+$ or $\mathcal{L}$:

$$\begin{aligned} \mathcal{L}^+\mathcal{L} = f(H_1) = \prod_{i=1}^{i=3}(H_1 - \epsilon_i), \qquad & \mathcal{L}\psi_i = 0, \quad H_1\psi_i = \epsilon_i, \\ \mathcal{L}\mathcal{L}^+ = g(H_1) = \prod_{i=1}^{i=3}(H_1 - \tilde{\epsilon}_i), \qquad & \mathcal{L}^+\tilde{\psi}_i = 0, \quad H_1\tilde{\psi}_i = \tilde{\epsilon}_i. \end{aligned} \tag{21}$$

Since

$$\mathcal{L}(\mathcal{L}^+\mathcal{L}) = \mathcal{L}f(H_1) = f(H_1 - 2)\mathcal{L} = (\mathcal{L}\mathcal{L}^+)\mathcal{L} = g(H_1)\mathcal{L} \tag{22}$$

we have that

$$\tilde{\epsilon}_i = \epsilon_i - 2, \qquad i = 1, 2, 3. \tag{23}$$

Now, we are in conditions to prove the following:

Property. If the irreducible (raising) DLO $\mathcal{L}$ annihilates the eigenfunction ψ with eigenvalue ϵ, $H_1\psi = \epsilon\psi$, then the lowering operator $\mathcal{L}^+$ will annihilate an eigenfunction $\tilde{\psi}$ with eigenvalue $\tilde{\epsilon} = \epsilon + 2$.

In order to prove this statement we have to build the eigenfunction $\tilde{\psi}$, satisfying these conditions. If $H_1\psi = \epsilon\psi$, we can build a second linearly independent eigenfunction, $\psi^\perp$, with the same eigenvalue (for instance by means of the Liouville formula $\psi^\perp = \psi \int \psi^{-2}$). Then, as $\mathcal{L}$ is irreducible, $\mathcal{L}^+\psi^\perp := \tilde{\psi} \neq 0$, satisfies all the requirements.

Of course, this property can be read backwards: if the irreducible (lowering) DLO $\mathcal{L}^+$ annihilates the eigenfunction $\tilde{\psi}$ with eigenvalue $\tilde{\epsilon}$, $H_1\tilde{\psi} = \tilde{\epsilon}\tilde{\psi}$, then $\mathcal{L}$ will annihilate an eigenfunction ψ with eigenvalue $\epsilon = \tilde{\epsilon} - 2$. The property is trivially satisfied when $\mathcal{L}$ is reducible.

This property will be used later to characterize the eigenfunctions of H_1 spanning support spaces for the representation of the algebra generated by $\{\mathcal{L}, \mathcal{L}^+\}$.

3.2. Closure relation and fourth Painlevé equation

As the chain (15) is not 'exactly closed', a continuation is possible applying successively the same transformations and taking care of the factorization energies[2]. As the intermediate intertwining relations $L_i H_i = H_{i+1} L_i$ (3) hold, $i = 1, 2, 3$, the double factorization (11) of each Hamiltonian in the chain

$$H_{i+1} = L_i L_i^+ + \alpha_i = L_{i+1}^+ L_{i+1} + \alpha_{i+1} \tag{24}$$

gives a system of three equations for the superpotentials [5]

$$f_2' + f_1' = f_1^2 - f_2^2 + \beta_1 \tag{25}$$

$$f_3' + f_2' = f_2^2 - f_3^2 + \beta_2 \tag{26}$$

[2] Note that some elements are shifted and some are not, for instance $L_4 = L_1$ and $\alpha_4 = \alpha_1 - 2$.

$$f_1' + f_3' = f_3^2 - f_1^2 + \beta_3 \tag{27}$$

where

$$\beta_i := \alpha_i - \alpha_{i+1} \tag{28}$$

and by definition[3] $\beta_1 + \beta_2 + \beta_3 = 2$. All the superpotentials can be written in terms of f_1 or better using new functions $g_i(x)$ defined as

$$g_i(x) := f_i(x) - x. \tag{29}$$

Then

$$f_2 = -\frac{g_1}{2} + \frac{g_1'}{2g_1} + \frac{\beta_2}{2g_1} \qquad \text{and} \qquad f_3 = -\frac{g_1}{2} - \frac{g_1'}{2g_1} - \frac{\beta_2}{2g_1}. \tag{30}$$

And the condition of the system to be solved is that g_1 fulfils Painlevé IV equation[4] [4–6, 8]:

$$gg'' = \tfrac{1}{2}(g')^2 + \tfrac{3}{2}g^4 + 4xg^3 + 2(x^2 - a)g^2 + b \tag{32}$$

with parameters

$$a = 1 - \beta_1 - \frac{\beta_2}{2} \qquad b = -\frac{1}{2}\beta_2^2. \tag{33}$$

Summarizing, the Hamiltonian H_1 admits a third-order DLO if it has a superpotential which provides, by means of (29), a solution of P_{IV}. The way back is also possible, i.e., each solution of P_{IV} generates a Hamiltonian with a third-order DLO.

Of course, the final P_{IV} equation associated with the third-order DLO is not unique: (i) each function g_i is solution of another P_{IV} and (ii) we can take other factorizations of the same DLO $\mathcal{L}$ leading to further P_{IV} equations. These features will be discussed in the following sections.

4. Hierarchies and geometrical representation

The relation between the third-order DLO and P_{IV} solutions is based on the factorization of the former: its chain representation. A DLO $\mathcal{L}$ is determined by the functions in its kernel, and depending on the order in which these functions are annihilated different factorizations are obtained [11, 23, 24]: up to 3! possibilities, which is also the number of new intermediate Hamiltonians. Starting from one cycle, with Hamiltonians $\{H_1, H_2, H_3\}$, we want to obtain the other five by means of certain operations.

The same operations can be applied to any of the cycles so obtained. In this way, the set of new Hamiltonians turns out to be infinite. All these Hamiltonians are said to belong to a hierarchy. The elements of each hierarchy can be considered into three layers: Hamiltonians with the third-order DLO, factorization eigenvalues and P_{IV} solutions.

In this section, two kinds of operations are defined: local and global, together with a geometrical representation that will help in understanding the structure of any hierarchy.

[3] Due to the invariance of the chain over addition of a global constant to the Hamiltonians, only eigenvalue differences are relevant. Since just two of the three eigenvalues are independent we will set the third one equal to zero.

[4] Without rescaling the equation for g_1 has the form

$$g_1 g_1'' = \tfrac{1}{2}(g_1')^2 + \tfrac{3}{2}g_1^4 + 2\gamma x g_1^3 + (\tfrac{\gamma^2}{2}x^2 + 2\beta_1 + \beta_2 - \gamma)g_1^2 - \tfrac{\beta_2^2}{2}. \tag{31}$$

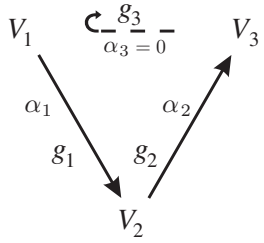

Figure 1. Three-step Darboux chain geometrical representation. The arrows show the direction of the 1-SUSY transformations.

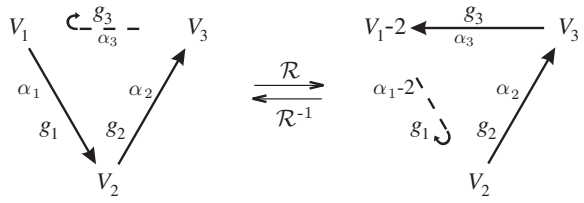

Figure 2. Geometrical representation of a cycle rotation.

4.1. Local operations: rotations and transpositions

Let us assume that H_1 is a Hamiltonian with a third-order DLO $\mathcal{L}_1$ (2) and we know one 3-SUSY cycle (15), denoted by C_1: $\{H_1, H_2, H_3\}$. A triangle representation is used to condense all the information (figure 1): in each vertex a potential (V_i) is placed. The arrows connecting vertexes have associated a factorization eigenvalue α_i (defining the 1-SUSY) and a P_{IV} solution g_i. Note that α_i's give the P_{IV} parameters through equations (28) and (33), and g_i's give the intermediate IO through equations (29) and (14).

In order to fix the first potential in the cycle, and also to keep track of the shift in some elements of the chain, the last arrow has a different shape and will be called *reference arrow*. For instance, after this arrow we read: $V_1 - 2, \alpha_1 - 2, V_2 - 2, \ldots$ and so on to continue the (pseudo)-cycle. As a criteria for a better understanding of symmetry properties in the geometrical representation we will choose $\alpha_3 = 0$ (see footnote 3) and place the reference arrow parallel to the horizontal axis.

4.1.1. Rotations. As a cycle does not exactly close and can be continued forward and backward it should be represented like a helix, but it is simpler to draw it like a loop in a plane just taking care of the shifts in H_i, V_i, α_i. Due to this continuation it is obvious that each intermediate Hamiltonian admits a third-order ladder operator, their cycles have no new elements. It is like choosing a new starting point, for instance, $C_2 : \{H_2, H_3, H_1 - 2\} \sim \{H_2; \alpha_2, \alpha_3, \alpha_1 - 2\} \sim \{H_2; g_2, g_3, g_1\}$.

We will refer to this operation by $\mathcal{R}$ and its geometrical effect will be an anticlockwise rotation of the arrows, making the necessary shifts ± 2 as shown in figure 2.

From the geometrical point of view, the rotations will be used to place the reference arrow of the triangles on the horizontal axis and show up better the symmetry properties in different

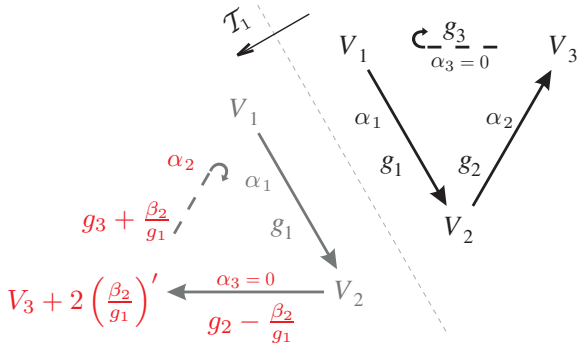

Figure 3. Diagram of $\mathcal{T}_1$ transformation: (*a*) eigenvalues are crossed, (*b*) P_{IV} solutions are modified adding a term proportional to $(\alpha_2 - \alpha_3)$ and to the inverse of g_1, (*c*) the third potential has an additional derivative term.

hierarchies. Summarizing the effect of $\mathcal{R}$ on C_1:

$$\begin{array}{lcl} & \mathcal{R} & \\ \mathcal{L}_1 = L_3L_2L_1 & \longrightarrow & \mathcal{L}_2 = L_1L_3L_2 \\ \{\alpha_1, \alpha_2, \alpha_3\} & \longrightarrow & \{\alpha_2, \alpha_3, \alpha_1 - 2\} \\ \{V_1, V_2, V_3\} & \longrightarrow & \{V_2, V_3, V_1 - 2\} \\ \{a_1, b_1\} & \longrightarrow & \left\{a_2 = 1 - \beta_2 - \frac{1}{2}\beta_3, b_2 = -\frac{1}{2}\beta_3^2\right\}. \end{array} \tag{34}$$

The superpotentials, g_i's, and the parameters β_i's are just affected by a cyclic rotation. Note that the solution g_2 of the 'rotated' P_{IV} equation can be written as a function of g_1 (30). Three consecutive applications of $\mathcal{R}$ gives a global shifted cycle, then $\mathcal{R}^3 \equiv \mathrm{I}$. Although the inverse rotation $\mathcal{R}^{-1}$ is equivalent to a double rotation $\mathcal{R}^2$ we will consider it as a positive shift on Hamiltonians and eigenvalues: $\mathcal{R}^{-1}C_1 \to C_0$, where $C_0 \sim \{H_3 + 2, H_1, H_2\} \sim \{\alpha_3 + 2, \alpha_1, \alpha_2\}$.

4.1.2. Transpositions. A factorization of $\mathcal{L}$ is determined by the annihilation order of the eigenfunctions with factorization eigenvalues $\{\alpha_1, \alpha_2, \alpha_3\}$ by the 1-SUSY IOs. Changing the annihilation order of the eigenfunctions associated to the last two eigenvalues gives the same $\mathcal{L}$ for H_1 but with different factorization and, therefore, with a new cycle [11, 23, 24]. All the elements of the new cycle can be expressed as functions of those of the old one. As the first eigenvalue is left invariant we will refer to this operation by $\mathcal{T}_1$. The application of $\mathcal{T}_1$ on C_1 gives, having in mind (30):

$$\begin{array}{lcl} & \mathcal{T}_1 & \\ \{\alpha_1, \alpha_2, \alpha_3\} & \longrightarrow & \{\alpha_1, \alpha_3, \alpha_2\} \\ \{V_1, V_2, V_3\} & \longrightarrow & \left\{V_1, V_2, V_3 + 2\left(\dfrac{\beta_2}{g_1}\right)'\right\} \\ \{g_1, g_2, g_3\} & \longrightarrow & \left\{g_1, g_2 - \dfrac{\beta_2}{g_1}, g_3 + \dfrac{\beta_2}{g_1}\right\}, \end{array} \tag{35}$$

where prime denotes differentiation.

Regarding geometry, $\mathcal{T}_1$ behaves like a reflection with respect to a parallel line to the first arrow since the elements on this line are left unchanged, as explained in figure 3. Transpositions are transformations of second order, i.e., $\mathcal{T}_1^2 \equiv \mathrm{I}$.

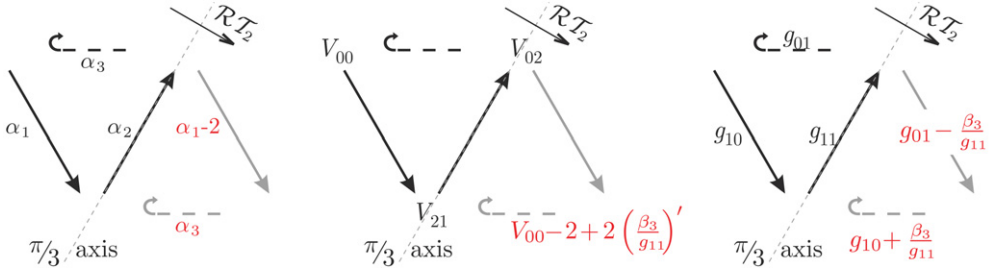

Figure 4. The transformation $\mathcal{R}\mathcal{T}_2$. Each picture shows the transformation rules of one element: factorization eigenvalues, potentials and P_{IV} solutions. The inverse $\mathcal{T}_2\mathcal{R}^{-1}$ recovers the starting cycle.

The operations $\mathcal{R}$ and $\mathcal{T}_1$ will be considered the basic ones. They do not commute and generate an infinite group of transformations. The relation between them is expressed by the identity

$$(\mathcal{R}\mathcal{T}_1\mathcal{R}^{-1}\mathcal{T}_1)^3 = \mathrm{I}. \tag{36}$$

Then, starting from a Darboux cycle, by applying these operations we can relate it with an infinite number of different cycles leading to a hierarchy of infinite Hamiltonians, each of them with a third-order shift operator, and also to a hierarchy of P_{IV} equations [9, 11, 25] whose solutions are also related.

We could have done a direct definition, in the same way as above, of two other transpositions $\mathcal{T}_2$ and $\mathcal{T}_3$ leaving unchanged the second and third arrow, respectively. However, it is also possible to define them combining the two operations already defined:

$$\mathcal{T}_2 := \mathcal{R}^{-1}\mathcal{T}_1\mathcal{R} \qquad \text{and} \qquad \mathcal{T}_3 := \mathcal{R}\mathcal{T}_1\mathcal{R}^{-1}. \tag{37}$$

In order to build the general geometrical structure of hierarchies, three transformation axis are defined using combinations of transpositions and rotations. An imaginary square grid is used to label potentials and P_{IV} solutions where an overline means a negative index. From now on potential V_{00}, equivalent to V_1, will be the starting potential set at the origin of the grid.

(i) $\frac{\pi}{3}$*-axis.* It forms a $\frac{\pi}{3}$ angle with the horizontal line and is related to $\mathcal{T}_2$ because this transformation leaves invariant the second arrow in the cycle. Besides $\mathcal{T}_2$, it is also necessary to apply a rotation to place the reference arrow on the horizontal axis. Then, we will assume that reflection with respect to the $\frac{\pi}{3}$-axis carries out the operation $\mathcal{R}\mathcal{T}_2$ when going from the upper plane to the lower one as seen in figure 4. Its inverse operation is $\mathcal{T}_2\mathcal{R}^{-1}$.

(ii) $-\frac{\pi}{3}$*-axis.* In this case the angle with the horizontal line is $-\frac{\pi}{3}$, the first arrow is invariant and we also need a rotation. Then, the transformation $\mathcal{R}^{-1}\mathcal{T}_1$ is used to go from the upper to the lower half-plane of the $-\frac{\pi}{3}$-axis (figure 5). Note that due to the rotation the first arrow is transformed into the second one of the new cycle.

(iii) *Horizontal axis*. The transformation is directly carried out by $\mathcal{T}_3$ (figure 6).

With these axes and their associated operations above defined, it is possible to find the other five cycles related to the starting Hamiltonian $H_1 \equiv H_{00}$ (15). It turns out to form a hexagon with the initial potential in the centre (figure 7). This fundamental cell in the geometrical representation of cycles is related to the commutation relation (36).

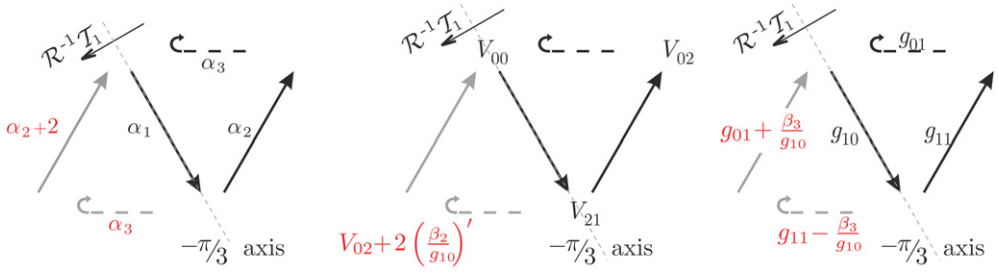

Figure 5. Scheme of $\mathcal{R}^{-1}\mathcal{T}_1$ transformation. The inverse is $\mathcal{T}_1\mathcal{R}$.

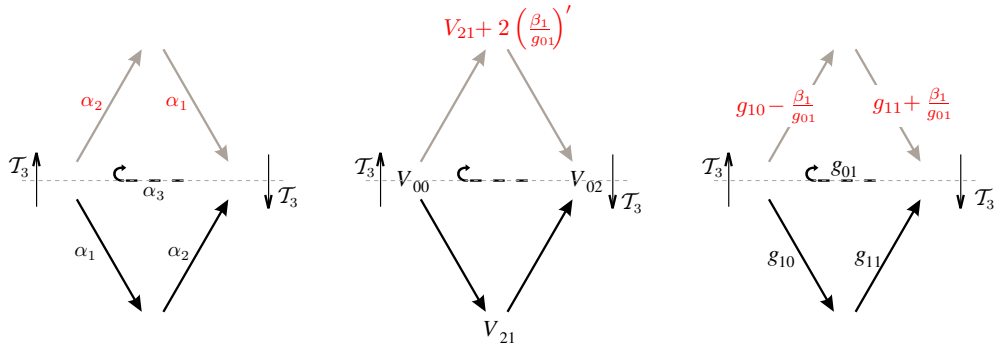

Figure 6. $\mathcal{T}_3$ transformation representation.

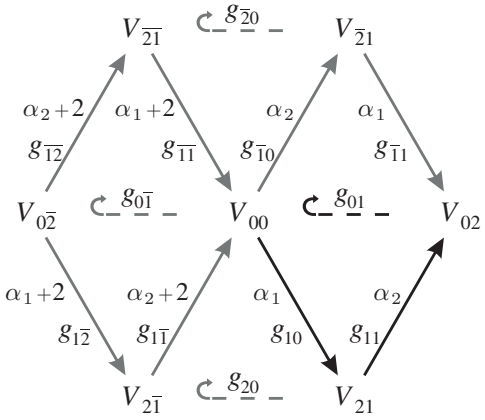

Figure 7. Representation of the six possible cycles associated with a Hamiltonian with potential V_{00}.

The hexagon (figure 7) involves up to 7 different potentials and 12 P_{IV} solutions all of them obtained from H_{00} and $g_{10} \equiv g_1$. The most interesting point is that these P_{IV} solutions are only generated by means of algebraic manipulations from $\{g_1, g_2, g_3\}$ of the initial cycle. For new potentials one differentiation is needed in each operation, or by means of P_{IV} solutions through superpotentials (6) just one differentiation is enough to compute any potential in the hierarchy.

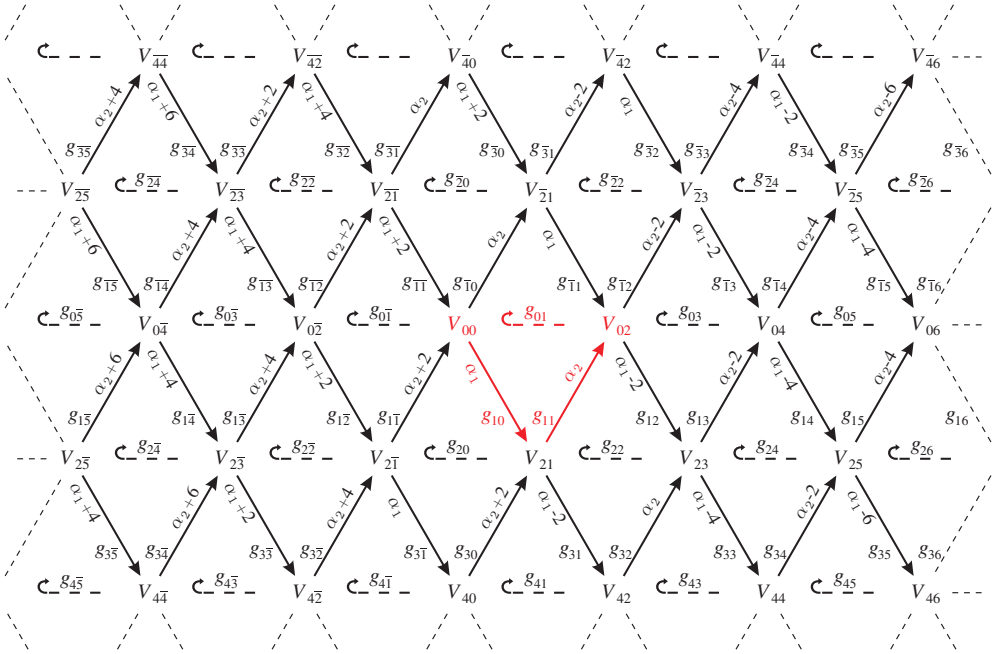

Figure 8. Diagram for an arbitrary hierarchy generated from one given cycle V_{00}, V_{21}, V_{02} (in red). Potentials, P_{IV} solutions and factorization eigenvalues are displayed.

4.2. Global operations: transfers

The basic operations are enough to cover the whole plane with triangles representing the cycles of a hierarchy, but it will be easier if we define transfer operations that enable us to move directly between neighbouring triangles (cycles) along the three reference axes ($\frac{\pi}{3}, -\frac{\pi}{3}$ and horizontal). Regarding the eigenvalues, as the third one is always set to zero and its associated arrow (the reference one) is placed on the horizontal axis, the other two axes $\left(\frac{\pi}{3}, -\frac{\pi}{3}\right)$ can be seen as eigenvalue axes. Therefore, we define two operations that just shift one eigenvalue (α_1 or α_2) leaving unchanged the others:

- Transfer along the $-\frac{\pi}{3}$-axis is carried out by $\mathcal{D}_1$

$$\mathcal{D}_1 := \mathcal{T}_3\mathcal{T}_1\mathcal{R} : \{\alpha_1, \alpha_2, \alpha_3\} \to \{\alpha_1 - 2, \alpha_2, \alpha_3\} \tag{38}$$

  changing the value of α_1 in steps of ± 2 units. The triangle arrows point at the decreasing direction.
- In the same way, transfer $\mathcal{D}_2$ changes α_2 along the $\frac{\pi}{3}$-axis,

$$\mathcal{D}_2 := \mathcal{T}_1\mathcal{R}\mathcal{T}_3 : \{\alpha_1, \alpha_2, \alpha_3\} \to \{\alpha_1, \alpha_2 - 2, \alpha_3\}. \tag{39}$$

Transfers $\mathcal{D}_3$ along the horizontal axis can be achieved applying a simultaneous shift along the other two axes, but it plays a secondary role. It is also possible to write $\mathcal{D}_2 = \mathcal{R}^{-1}\mathcal{D}_1\mathcal{R}$ and $\mathcal{D}_3 = \mathcal{R}\mathcal{D}_1\mathcal{R}^{-1}$.

The most general hierarchy's structure is shown in figure 8. In particular, it can be seen how factorization eigenvalues are distributed, which will be a very useful tool to analyse the structure of particular hierarchies, the spectrum and singularities of the generated potentials and P_{IV} solutions, and how these properties are periodically distributed in hierarchies.

4.3. Fundamental cell in eigenvalue space

We have seen that all the eigenvalues involved in a hierarchy can be derived through application of basic operations from a starting pair (α_1, α_2), then each hierarchy has a set of related pairs of eigenvalues and can be characterized giving the value of one of those pairs (note that we have fixed $\alpha_3 = 0$). Thus, considering the space of eigenvalues $\mathbb{R}^2$ we can find a fundamental cell where each point (α_1, α_2) determines a different hierarchy.

Moreover, each hierarchy has associated a set of P_{IV} equations (32) whose parameters are determined by the factorization eigenvalues (33). Then, the problem of solving a P_{IV} with arbitrary parameters is 'reduced' to find the solutions of the P_{IV} equations whose parameters lie in the fundamental cell. In particular, some special values of the cell parameters will be shown to have simple rational solutions.

The (real) factorization eigenvalues (α_1, α_2) will be represented as the Cartesian coordinates in the affine $\mathbb{R}^2$ eigenvalue space. Any operation will be represented by an affine transformation. The action of a rotation $\mathcal{R}$ is (section 4.1)

$$\{\alpha_1, \alpha_2, 0\} \quad \xrightarrow{\mathcal{R}} \quad \{\alpha_2, 0, \alpha_1 - 2\} \equiv \{\alpha_2 - \alpha_1 + 2, -\alpha_1 + 2, 0\}, \tag{40}$$

so, its affine matrix, acting on the vector $\{1, \alpha_1, \alpha_2\}$, is

$$\mathcal{R} = \begin{pmatrix} 1 & 0 & 0 \\ 2 & -1 & 1 \\ 2 & -1 & 0 \end{pmatrix}. \tag{41}$$

In a similar way the matrix for $\mathcal{T}_1$ is

$$\mathcal{T}_1 = \begin{pmatrix} 1 & 0 & 0 \\ 0 & 1 & -1 \\ 0 & 0 & -1 \end{pmatrix}. \tag{42}$$

And from these two matrices we can get all the operations. In order to obtain the fundamental cell it is useful to write down the following matrices:

$$\mathcal{T}_3 = \begin{pmatrix} 1 & 0 & 0 \\ 0 & 0 & 1 \\ 0 & 1 & 0 \end{pmatrix} \qquad \mathcal{D}_1 = \begin{pmatrix} 1 & 0 & 0 \\ -2 & 1 & 0 \\ 0 & 0 & 1 \end{pmatrix} \qquad \mathcal{D}_2 = \begin{pmatrix} 1 & 0 & 0 \\ 0 & 1 & 0 \\ -2 & 0 & 1 \end{pmatrix}. \tag{43}$$

By means of the transfer matrices $\mathcal{D}_1$ and $\mathcal{D}_2$ the whole eigenvalue space is obtained from a square cell of size 2×2 because they perform a displacement of two units in each axis: factorization eigenvalues $\{\alpha_1 - 2n, \alpha_2 - 2m, 0\}$ with $m, n \in \mathbb{Z}$ belong to the same hierarchy. Now, as $\mathcal{T}_3$ is a reflection through the bisector of the axes, the square cell is reduced to a rectangular triangle (figure 9): $\{\alpha_1, \alpha_2, 0\}$ such that $0 \leqslant \alpha_2 < \alpha_1 < 2$.

Finally, the symmetry under $\mathcal{R}$ has to be explored. Note that in this space distance is not conserved and $\mathcal{R}$ is not a proper rotation (41), but as $\mathcal{R}^3$ is the identity the rectangular triangle is divided into three (irregular) triangles. There is only one invariant point under $\mathcal{R}$, which is $\left\{\frac{4}{3}, \frac{2}{3}\right\}$. Joining each vertex of the previous rectangular triangle with this point gives the new irregular triangles shown in figure 9.

Each triangle can be used as the definition of the fundamental cell. We choose the one with basis on α_1 axis. Then, the fundamental cell is the set of points

$$\left\{(\alpha_1, \alpha_2) \in \mathbb{R}^2 / \alpha_2 \in \left[0, \tfrac{1}{2}\alpha_1\right], \alpha_1 \in \left[0, \tfrac{4}{3}\right]; \alpha_2 \in (0, 2 - \alpha_1), \alpha_1 \in \left(\tfrac{4}{3}, 2\right)\right\}. \tag{44}$$

Any hierarchy is determined giving one point within this triangle, for instance, sets of points belonging to three different hierarchies are shown in figure 9.

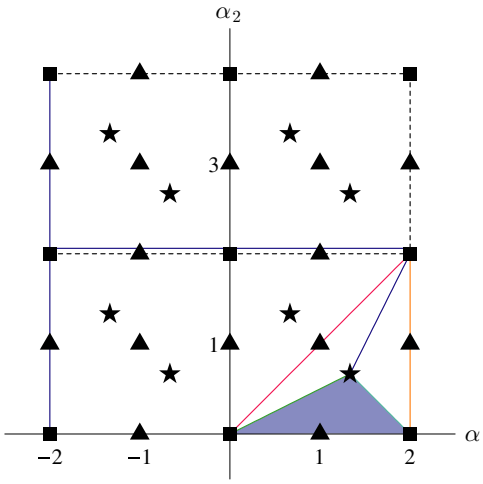

Figure 9. Fundamental cell. Points with the same shape represent cycles in the same hierarchy: squares for hyperconfluent, triangles for confluent and stars for rotational. They have been generated from the ones within the fundamental cell.

The parameters of P_{IV} equations in the same hierarchy are grouped into three sets:

$$\begin{aligned} a &= 1-\alpha_1+\frac{\alpha_2}{2}+m-2n; \qquad & b &= -\frac{1}{2}(\alpha_2+2m)^2 \\ a &= 1+\frac{\alpha_1}{2}-\alpha_2+m-2n; \qquad & b &= -\frac{1}{2}(\alpha_1+2m)^2 \\ a &= 1+\frac{\alpha_1+\alpha_2}{2}+m-2n; \qquad & b &= -\frac{1}{2}(\alpha_1-\alpha_2+2m)^2 \end{aligned} \tag{45}$$

with α_1 and α_2 in the fundamental cell and $m, n \in \mathbb{Z}$.

4.4. Group structure

In this section, we have introduced some basic operations on the cycles composing a hierarchy. These transformations have the structure of an infinite group generated by $\mathcal{R}$ and $\mathcal{T}_1$. We can characterize this group from a geometrical point of view inside the affine two-dimensional plane: $\mathcal{R}$ is represented by a three-fold rotation and $\mathcal{T}_1$ by a reflection with respect to a line not including the centre of rotation.

The subgroup made of reflections has reflection axes parallel to the three lines mentioned above: $\frac{\pi}{3}, -\frac{\pi}{3}$ and horizontal axes. It can be shown that this is an affine reflection group isomorphic to $\widetilde{A}_2$ [5, 26, 27]. The subgroup $\mathbb{Z}_3$ generated by $\mathcal{R}$ is represented by rotations around the centre of an elemental triangle formed by three reflection axes. An element of $\mathbb{Z}_3$ fixes the starting point of the cycle corresponding to such a triangle. Thus, we can say that the whole transformation group has the structure of semidirect product of the invariant subgroup $\widetilde{A}_2$ and the rotation subgroup $\mathbb{Z}_3$ [26].

5. Harmonic oscillator hierarchies

The invariance under some basic operations simplify the general hierarchy giving rise to more symmetrical structures. The harmonic oscillator (HO) is in the background of this situation and at the same time it supplies us with solutions of P_{IV} that can be expressed in terms of

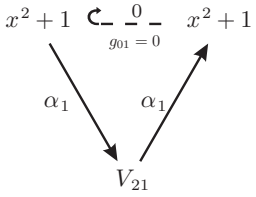

Figure 10. General three-step cycle for the harmonic oscillator generated by means of an arbitrary 1-SUSY partner.

hypergeometric functions. Bassom *et al* in [9] have shown three hierarchies including this type of functions, which were obtained by the application of different Bäcklund transformations. Here, we will see how all of them are related to the harmonic oscillator and fit quite well in our approach. Besides, we will study some properties of the physical spectrum of the generated Hamiltonians in these hierarchies.

Since the harmonic oscillator has a first-order DLO any of its 1-SUSY partners enables the construction of a three-step Darboux chain (figure 10). The cycle is built using two identical energies $\alpha_1 = \alpha_2$, needed for the 1-SUSY relation, and the ground-physical energy for the HO first-order DLO (which will be taken $\alpha_3 = 0$). These factorization eigenvalues in the fundamental cell correspond to the bottom line (figure 9). The above-mentioned three types of hierarchies [9] are related to the factorization properties of $\mathcal{L}$ (section 3.1) and characterized as follows:

Hyperconfluent hierarchy. It is the simplest hierarchy, defined by the point $\{0, 0\}$ in figure 9. The same eigenvalue $\alpha_1 = \alpha_2 = \alpha_3 = 0$ is used in the factorization providing a realization of diagram (17), hence the name of HO hyperconfluent hierarchy. In this case, the general scheme (figure 8) has several additional global symmetries (see figure 11). To show them clearly we have applied transpositions without rotations, finding three reflection symmetries: $\mathcal{T}_3$ leaves invariant one horizontal line, $\mathcal{T}_1$ one $\frac{\pi}{3}$ line and $\mathcal{T}_2$ one $-\frac{\pi}{3}$ line. Each symmetry divides the hierarchy into two halves generating six identical wedges. The starting hexagon has six identical cycles (figure 11) and each square in figure 9 includes just one point.

Confluent hierarchy. For the other points lying in the bottom line of the fundamental eigenvalue cell $\{\alpha, 0\}, \alpha \in (0, 2)$, there is also a global symmetry in the general scheme (figure 8). In this case, only the reflection $\mathcal{T}_3$ in one horizontal line divides the hierarchy into two identical parts (figure 20), thus the starting hexagon has just three different cycles (three points in each square in figure 9). This class supplies a realization of the confluent case of section 3.1.

Rotational hierarchy. One more hierarchy is known to be associated with the HO. It is obtained by repeated application of the first-order HO ladder operator. And it is characterized by the rotational invariant point $\left\{\frac{4}{3}, \frac{2}{3}\right\}$ in the fundamental cell (figure 9), where two points are found in each square. Since the initial cycle has a rotational symmetry, this three-fold symmetry is inherited by the whole hierarchy as shown in figure 25. All the factorization eigenvalues are different so it constitutes a very special realization of the non-degenerated case of section 3.1.

In the following, we will consider the main features of each hierarchy type.

6. The hyperconfluent hierarchy

The harmonic oscillator potential $V(x) = x^2 + 1$ gives a one parameter family of starting cycles for this hierarchy. Any linear combination of eigenfunctions with eigenvalue $\alpha = 0$

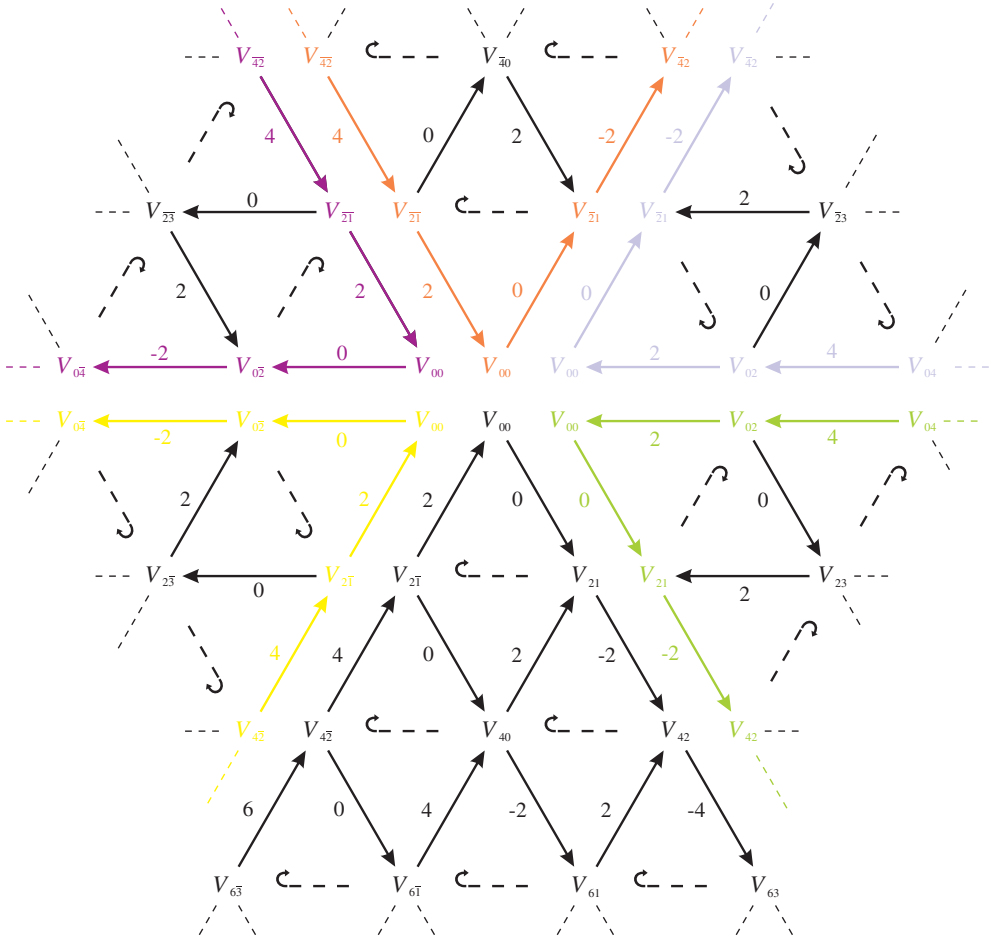

Figure 11. General diagram for the hyperconfluent hierarchy.

can be chosen, leading to two kinds of hyperconfluent hierarchies:

(i) Shifted HO: $u_1 = \mathrm{e}^{\frac{x^2}{2}}$.
(ii) Complementary error function[5]:

$$u_2 = \mathrm{e}^{\frac{x^2}{2}}(A + \mathrm{erfc}(x)) \equiv Q(x), \tag{46}$$

where A is an arbitrary constant.

Each one gives different solutions for the same $\mathrm{P_{IV}}$ with the same hierarchical structure and eigenvalues, but different potentials. We now show the properties of each hierarchy.

6.1. The shifted HO hyperconfluent hierarchy

The shifted harmonic oscillator $V_{21}(x) = x^2 - 1$ is the 1-SUSY partner of the HO in figure 10. We choose the central bottom wedge of figure 11 to represent this hierarchy then, we need to make a $-\frac{\pi}{3}$-axis transformation to build it (figure 12). This cycle is enough

[5] Where $\mathrm{erfc}(x) = \frac{2}{\sqrt{\pi}}\int_x^\infty \mathrm{e}^{-t^2}\,\mathrm{d}t$.

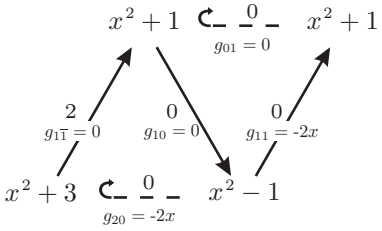

Figure 12. Starting cycle for the shifted harmonic oscillator hierarchy. Values of P_{IV} solutions are shown.

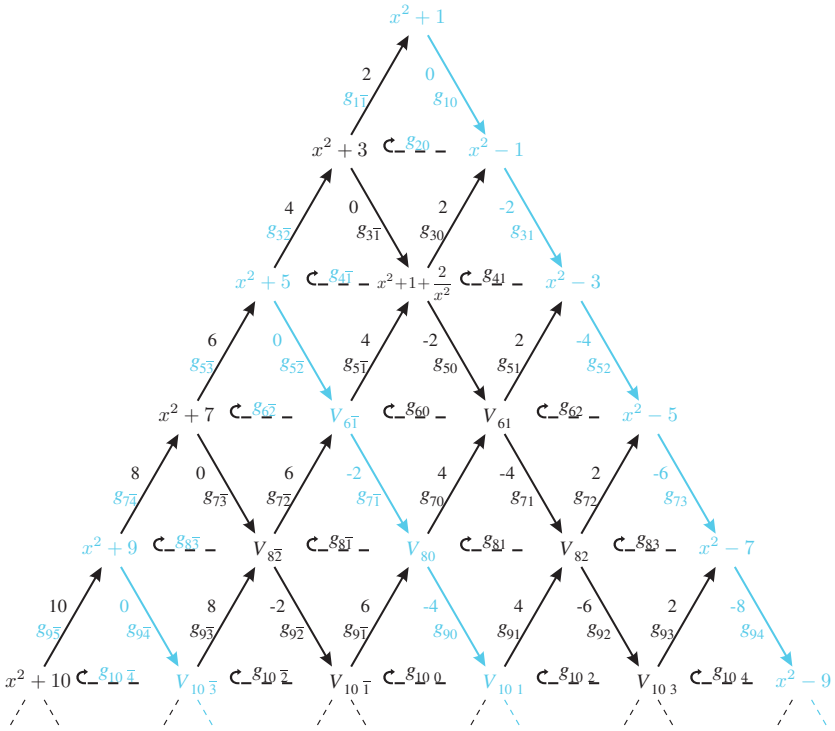

Figure 13. Scheme for shifted harmonic oscillator hierarchy.

to generate the whole hierarchy, whose potentials have the following properties:

(i) Potentials on both edges of the wedge are shifted HO potentials. On the left edge they are raised in steps of two units and on the right one they are lowered (figure 13).

(ii) Parallel lines to the right edge ($-\frac{\pi}{3}$-axis) are alternately filled with regular potentials with spectrum consisting of two sets of equispaced physical eigenvalues, one infinite and the other finite. As we go down in the hierarchy the finite set increases its size in one eigenvalue. Both sets are separated by another finite set of equispaced eigenvalues but associated with non-physical eigenfunctions. This last set is increased in two units as we move horizontally from the right edge to the left one.

These properties are easily explained in two ways using SUSY-QM results (section 2). Taking the right edge as a reference and following the horizontal line towards the left edge, the reasoning is based on the annihilation of levels. Note that in this edge the HO ground

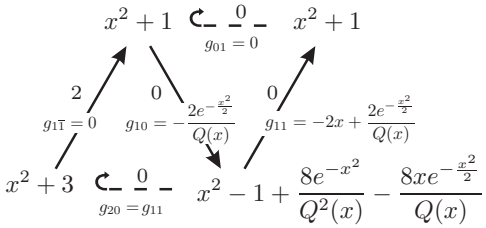

Figure 14. Starting cycle for the error function hierarchy. Values of P_{IV} solutions are shown.

level is placed below the zero eigenvalue. Then, a two-step movement represents a 2-SUSY transformation involving two consecutive energies that leads to a regular potential with these two levels removed from its spectrum (section 2) [3, 16]. The intermediate potential has singularities because of the vanishing points of the first 1-SUSY generating eigenfunction. Going on along the horizontal line another two levels are removed below the previous ones until we reach the left edge where the finite set have been removed.

On the other hand, in the left edge the ground state of the HO is placed above the zero eigenvalue. If we move downwards a $-\frac{\pi}{3}$ line, non-physical eigenfunctions are used to generate the 1-SUSY transformation. When there is an even number of levels between the ground energy and the zero energy the resulting potential is regular with a created new energy, otherwise it has singularities (section 2) [3, 16]. Then, we have alternatively $-\frac{\pi}{3}$ lines filled with regular and singular potentials. Moreover, going along a regular $-\frac{\pi}{3}$ line, one level below the previous one is created thus, the finite spectrum set is increased while the unphysical gap remains constant.

In summary, the spectrum of a potential in this wedge is characterized according to its position with respect to the two edges. The horizontal separation from the right edge indicates the gap between the finite and non-finite spectrum for regular potentials that must be even. The $-\frac{\pi}{3}$-axis separation of the left edge gives the number of bound states in the finite sector spectrum (figure 13).

6.2. The error function hyperconfluent hierarchy

The properties of the error function hierarchy, a one parameter family hierarchy fixed by $A \notin [-2, 0]$, are essentially the same as in the previous case. Similar arguments about the regular and singular behaviour apply. However, the potentials are not so simple, since the error function is present in the initial eigenfunction. The main difference is that, although the left edge has the same shifted HO potentials, the right edge is not filled with shifted HO's but with their isospectral potentials (figure 14).

P_{IV} solutions have similar regular properties in both hierarchies. Solutions 'connecting' regular potentials (alternate parallel $-\frac{\pi}{3}$ lines) are regular and increasing in two units the number of zeros in each step as going downwards. In the other series of parallel lines, the solutions have singularities, also increasing its number in two units.

Solutions associated with $\frac{\pi}{3}$ parallel lines are all singular but the null trivial solution coinciding with the left edge. The number of singularities is equal in each line and increases in one unit as the line moves away from the left edge.

For solutions in horizontal lines it is seen that going down, along the $-\frac{\pi}{3}$ direction, the number of singularities increases in one unit each step. The same happens as we move on the horizontal direction from the left edge. Horizontal regular solutions are only found in the left edge triangles.

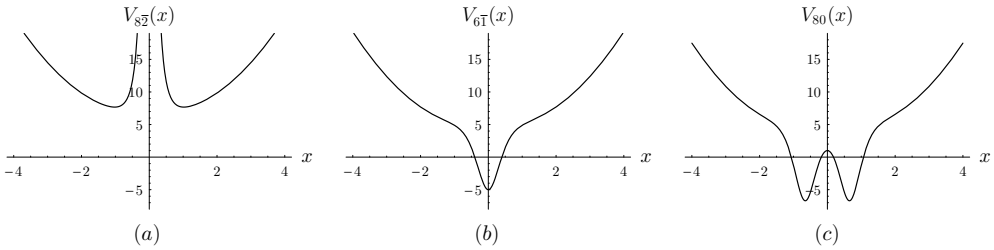

Figure 15. Potentials of the shifted HO hierarchy: (*a*) Potential $V_{8\bar{2}}(x)$ (*b*) potential $V_{6\bar{1}}(x)$ (*c*) potential $V_{80}(x)$.

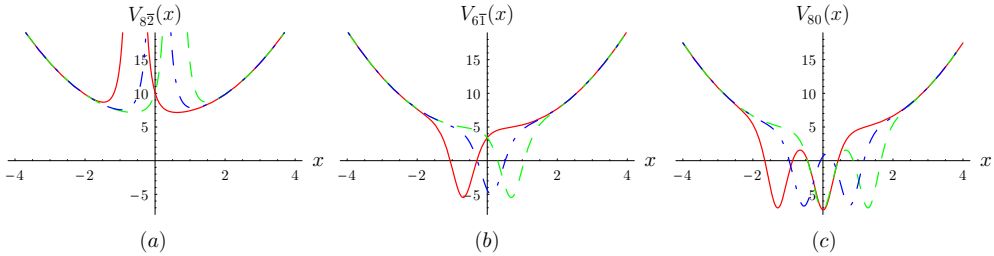

Figure 16. Potentials of the error function hierarchy with parameter $A = -2.1$ in red continuous, $A = 0.1$ in green dashed and $A = 3$ in blue dotted and dashed (*a*) potential $V_{8\bar{2}}(x)$ (*b*) potential $V_{6\bar{1}}(x)$ (*c*) potential $V_{80}(x)$.

The asymptotical behaviour of $\mathrm{P_{IV}}$ solutions on $\pm\frac{\pi}{3}$ lines is the same, vanishing as $x \to \pm\infty$. This effect comes from eigenfunctions that diverge at infinity. Contrary, the solutions on horizontal lines diverge as $x \to \pm\infty$, due to convergent vanishing eigenfunctions. Some examples are shown in section 6.3.

Another difference worth noting concerning the shifted HO hierarchy, is the existence of a parameter set, $A \in (-2, 0)$, where the regular and singular properties are swapped due to the error function shape: $-\frac{\pi}{3}$ lines which were filled with regular potentials and $\mathrm{P_{IV}}$ solutions are now singular and vice versa. When $A = -2$ or $A = 0$ the finite set in the spectrum of regular potentials disappears, remaining only the infinite one.

6.3. Examples

Let us work out an example to illustrate these properties. Consider the potential $V_{80}(x)$ in the cycle with factorization energies $\{6, -2, 0\}$, potentials $\{V_{8\bar{2}}, V_{6\bar{1}}, V_{80}\}$ and $\mathrm{P_{IV}}$ solutions $\{g_{7\bar{2}}, g_{7\bar{1}}, g_{8\bar{1}}\}$ (see figure 13).

Following the previous arguments it is easy to check the main properties. The first potential $V_{8\bar{2}}$ is separated by an odd number of steps from the right edge then, it is non-regular. As it is one step off the left edge it only has one singularity (figure 15–16(*a*)). The other two potentials lie on a $-\frac{\pi}{3}$ regular line so they have a physical spectrum. Both of them are two steps from the right edge then, there is a gap of two levels between the infinite and the finite equispaced spectra. The finite set has one point for $V_{6\bar{1}}$ and two points for V_{80} according to their separation from the left edge (figures 15–16(*b*) and (*c*)). It is also shown in figure 17 how the analysis is completely reversed when $A \in (-2, 0)$.

More explicitly, for the Hamiltonian with potential V_{80} we have[6]:

[6] All the explicit expressions in this section are given for the shifted HO hierarchy.

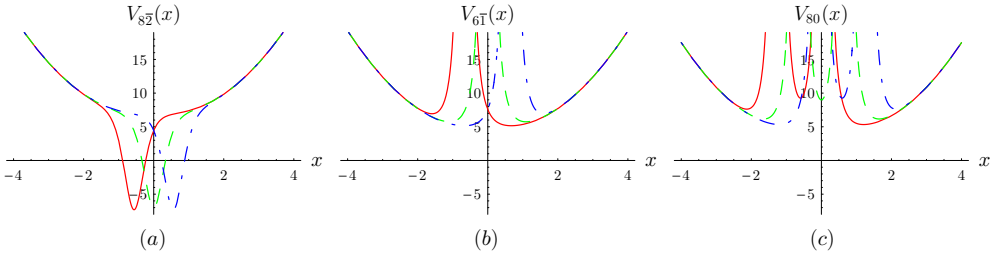

Figure 17. Potentials of the error function hierarchy with parameter $A = -1.9$ in red continuous, $A = -1$ in green dashed and $A = -0.1$ in blue dotted and dashed (*a*) potential $V_{8\bar{2}}(x)$ (*b*) potential $V_{6\bar{1}}(x)$ (*c*) potential $V_{80}(x)$.

(i) P_{IV} solutions for this cycle are obtained applying basic operations on the starting cycle $\{2, 0, 0\}$ (see figures 12, 14). First acting twice with the inverse of $\mathcal{D}_1$ (38), then once with transfer $\mathcal{D}_2$, and we are led to the cycle of energies $\{6, -2, 0\}$, where V_{80} is in the third position. Only algebraic manipulations are needed to achieve an explicit expression for $\{g_{7\bar{2}}, g_{7\bar{1}}, g_{8\bar{1}}\}$. All the information about V_{80} can be extracted from its related P_{IV} solutions, six in total: three associated with arrows pointing inwards, $g_{7\bar{1}}, g_{81}, g_{9\bar{1}}$ (see figure 13),

$$g_{7\bar{1}} = -\frac{4x}{1+2x^2} + \frac{16x^3}{3+4x^4} \tag{47}$$

$$g_{81} = -2x - \frac{1}{x} + \frac{4x}{3-2x^2} + \frac{16x^3}{3+4x^2} \tag{48}$$

$$g_{9\bar{1}} = -\frac{4x(27+72x^2+16x^8)}{-27+54x^2+96x^6+48x^8+32x^{10}} \tag{49}$$

and three pointing outwards, $g_{70}, g_{8\bar{1}}, g_{90}$ (see figure 13),

$$g_{70} = \frac{4x}{-1+2x^2} - \frac{16x^3}{3+4x^4} \tag{50}$$

$$g_{8\bar{1}} = -2x + \frac{1}{x} + \frac{4x}{3+2x^2} - \frac{16x^3}{3+4x^4} \tag{51}$$

$$g_{90} = \frac{4x(27-72x^2+16x^8)}{27+54x^2+96x^6-48x^8+32x^{10}}. \tag{52}$$

(ii) The potential V_{80} can be obtained in several ways, applying basic operations, but they involve one differentiation in each step. Or, using any of the related P_{IV} solutions where just one differentiation is involved: the superpotential is given by equation (29) and the potential is calculated with the help of equation (6) (for incoming arrows the superpotential sign is changed). This potential is

$$V_{80} = 1 + x^2 + \frac{32x^2(-9+4x^4)}{(3+4x^4)^2} \tag{53}$$

And, in the error function hierarchy it is a rational function involving $Q(x)$ (46).

(iii) The third-order ladder operator (12) is built up using P_{IV} solutions of a cycle properly ordered (47)–(51):

$$\mathcal{L}_{V_{80}} = (\partial_x - (g_{7\bar{1}} + x))(\partial_x - (g_{7\bar{2}} + x))(\partial_x - (g_{8\bar{1}} + x)). \tag{54}$$

It is a creation ladder operator and its adjoint (9) is the annihilation ladder operator.

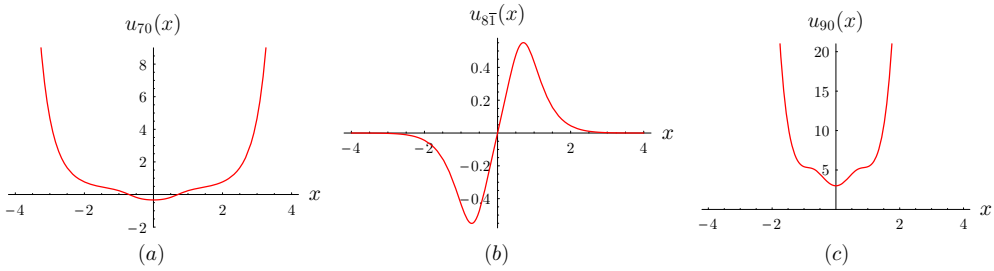

Figure 18. $V_{80}(x)$ eigenfunctions in the shifted HO hierarchy annihilated by creation third-order operator corresponding to the eigenvalues: -4 (a), 0 (b) and 4 (c).

(iv) The spectrum of square-integrable functions is found by means of the functions annihilated by the third-order ladder operators. So, the three functions annihilated by the creation operator are calculated from the P_{IV} outgoing solutions g_{70}, $g_{8\bar{1}}$ and g_{90} with eigenvalues 4, 0 and -4, respectively, through the superpotential definition (5). These solutions are

$$u_{70} = \frac{-1+2x^2}{3+4x^4}\,\mathrm{e}^{\frac{x^2}{2}} \tag{55}$$

$$u_{8\bar{1}} = \frac{x(3+2x^2)}{3+4x^4}\,\mathrm{e}^{\frac{-x^2}{2}} \tag{56}$$

$$u_{90} = \frac{9+18x^2-12x^4+8x^6}{3+4x^4}\,\mathrm{e}^{\frac{x^2}{2}}. \tag{57}$$

They correspond to the top level of three different eigenfunction sets, each one with the same character: u_{70} and u_{90} are not square-integrable, while $u_{8\bar{1}}$ is (figure 18).
The lowering third-order operator annihilates other three functions. These are obtained from the P_{IV} incoming solutions $g_{7\bar{1}}$, g_{81} and $g_{9\bar{1}}$ with eigenvalues -2, 2 and 6, respectively. They are

$$u_{7\bar{1}} = \frac{1+2x^2}{3+4x^4}\,\mathrm{e}^{\frac{-x^2}{2}} \tag{58}$$

$$u_{81} = \frac{x(-3+2x^2)}{3+4x^4}\,\mathrm{e}^{\frac{x^2}{2}} \tag{59}$$

$$u_{9\bar{1}} = \frac{-9+18x^2+12x^4+8x^6}{3+4x^4}\,\mathrm{e}^{\frac{-x^2}{2}}. \tag{60}$$

Now, these eigenfunctions correspond to the lowest level of three eigenfunction sets, each one including eigenfunctions with the same character: $u_{7\bar{1}}$ and $u_{9\bar{1}}$ are square-integrable while u_{81} is not (figure 19).

From these results we conclude that the spectrum consists of two sets of eigenvalues

$$\mathcal{E} = \{-2, 0\} \cup \{6, 8, \ldots, 2n \ldots\}. \tag{61}$$

That is, a finite set with two eigenvalues and an infinite one separated by a gap of two non-physical eigenvalues.

From the point of view of the algebra $\{H, \mathcal{L}^{\pm}\}$, these eigenfunctions generate the support spaces of four irreducible representations: two of them are non-physical (made up of non-square-integrable functions) corresponding to the eigenvalue sets $\mathcal{E}_1 = \{\ldots, -2m, \ldots, -4\}, \mathcal{E}_2 = \{2, 4\}$; and two physical: $\mathcal{E}_3 = \{-2, 0\}, \mathcal{E}_4 = \{6, 8, \ldots, 2n \ldots\}$.

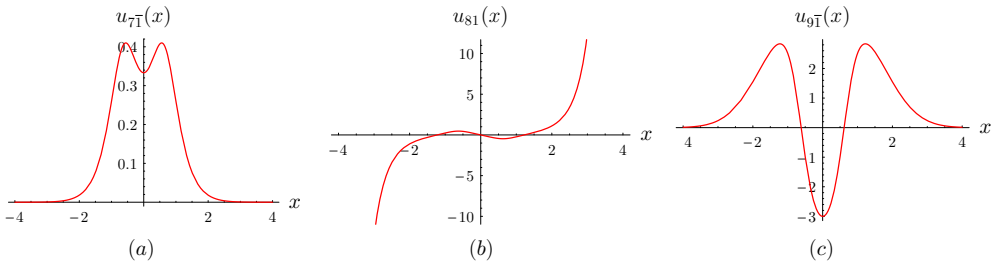

Figure 19. $V_{80}(x)$ eigenfunctions in the shifted HO hierarchy annihilated by annihilation third-order operator with eigenvalues: -2 (a), 2 (b) and 6 (c).

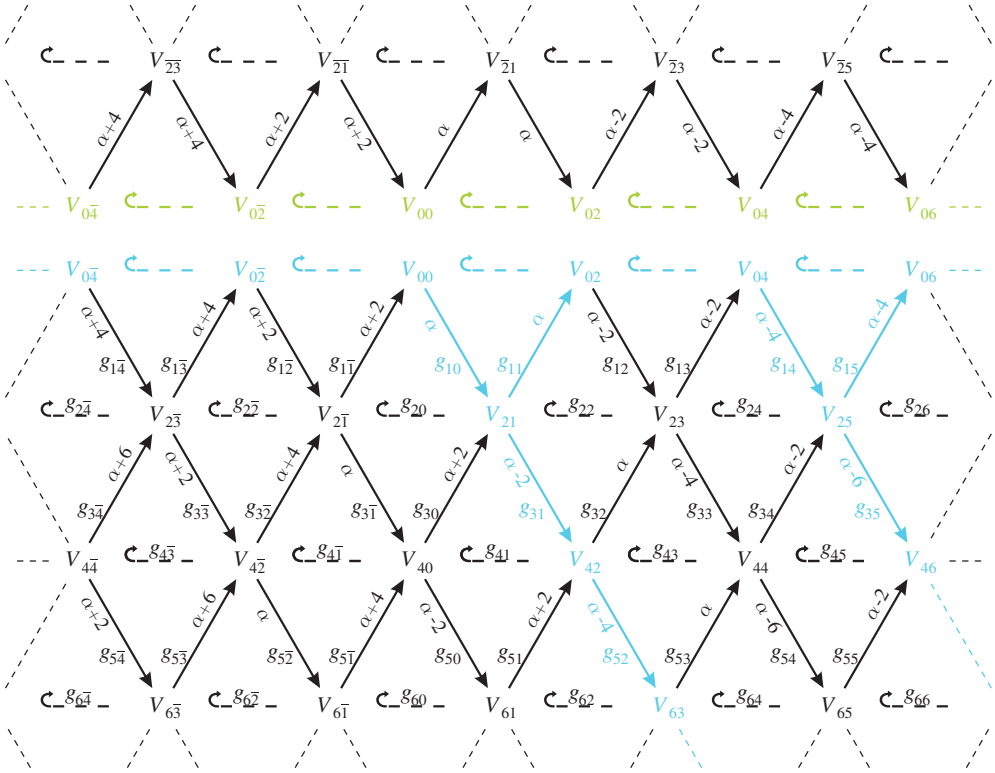

Figure 20. General scheme showing the invariant horizontal line under $\mathcal{T}_3$ for the confluent hierarchy: $\{\alpha, 0\}$.

Exactly the same situation occurs in the error function hierarchy when $A \notin [-2, 0]$ with more complicated expressions. When $A \in (-2, 0)$ the potential V_{80} is non-regular then, the whole spectral analysis is nonsense, but the same procedure can be applied to other regular potentials in the hierarchy.

7. The confluent hierarchy

Let us consider the more general but less symmetrical confluent hierarchy. In the general scheme (figure 20) it has one global horizontal symmetry axis. The simplest starting cycle

for a general $\alpha \in (0, 2)$ is shown in figure 10. There are two independent solutions for the HO eigenvalue problem that can be written in terms of confluent hypergeometric functions: $e^{-x^2/2}\Phi\left(\frac{2-\alpha}{4}; \frac{1}{2}; x^2\right)$ and $e^{-x^2/2}x\Phi\left(1-\frac{\alpha}{4}; \frac{3}{2}; x^2\right)$. Any linear combination of them generates a solution of P_{IV} with parameters $a = 1 - \frac{\alpha}{2}$, $b = -\frac{1}{2}\alpha^2$ leading to a one parameter family of P_{IV} solutions.

Consider the general eigenfunction[7] [28, 29]

$$u_\alpha(x) = e^{-\frac{x^2}{2}}\left[D\Phi\left(\frac{2-\alpha}{4}; \frac{1}{2}; x^2\right) + x\Phi\left(1-\frac{\alpha}{4}; \frac{3}{2}; x^2\right)\right]. \tag{62}$$

It gives rise to the first P_{IV} solutions of the starting cycle $C_1 : \{H_{00}, H_{21}, H_{02}\}$ through equations (5) and (29):

$$\begin{aligned}
g_{10}(x) &= -2x + \frac{(\alpha-2)\left(\Phi\left(1-\frac{\alpha}{4}; \frac{3}{2}; x^2\right) - 2Dx\Phi\left(\frac{3}{2}-\frac{\alpha}{4}; \frac{3}{2}; x^2\right)\right) - (\alpha-4)\Phi\left(2-\frac{\alpha}{4}; \frac{3}{2}; x^2\right)}{2\left(D\Phi\left(\frac{2-\alpha}{4}; \frac{1}{2}; x^2\right) + x\Phi\left(1-\frac{\alpha}{4}; \frac{3}{2}; x^2\right)\right)} \\
g_{11}(x) &= -\frac{(\alpha-2)\left(\Phi\left(1-\frac{\alpha}{4}; \frac{3}{2}; x^2\right) - 2Dx\Phi\left(\frac{3}{2}-\frac{\alpha}{4}; \frac{3}{2}; x^2\right)\right) - (\alpha-4)\Phi\left(2-\frac{\alpha}{4}; \frac{3}{2}; x^2\right)}{2\left(D\Phi\left(\frac{2-\alpha}{4}; \frac{1}{2}; x^2\right) + x\Phi\left(1-\frac{\alpha}{4}; \frac{3}{2}; x^2\right)\right)} \\
g_{01}(x) &= 0.
\end{aligned} \tag{63}$$

The behaviour of the eigenfunction $u_\alpha(x)$ (62) leads to three different situations related to its vanishing points. Two parameter regions are separated by an α-dependent value [29] $D_{\lim} := \frac{\Gamma(\frac{2-\alpha}{4})}{2\Gamma(1-\frac{\alpha}{4})}$: (i) there are no vanishing points if $D \in (D_{\lim}, \infty)$ then $u_\alpha(x) \to +\infty$ as $|x| \to \infty$; (ii) if $D \in [0, D_{\lim})$ there is one zero and the function goes to $\pm\infty$ as $x \to \pm\infty$; and finally (iii) when $D = D_{\lim}$ the function goes asymptotically to zero as $x \to -\infty$ and diverges to ∞ when $x \to \infty$. In analogy to the error function hyperconfluent hierarchy the properties of the situations (i) and (ii) are similar but the regular and singular potentials of parallel $-\frac{\pi}{3}$ lines are interchanged while case (iii) gives isospectral potentials. We will fix our attention on the first situation (i).

Due to the global symmetry, we can restrict to the lower half plane of the hierarchy, which is obtained by applying basic operations to the starting cycle (figure 10) as described in the previous section. To study the regularity properties the $-\frac{\pi}{3}$ lines will act as reference and, in particular, the one crossing V_{00} will play the role of a border line.

The properties of the potentials in this hierarchy are the following:

(i) Potentials on the top horizontal line consist of the same HO potential $V(x) = x^2 + 1$.

(ii) Regular potentials are placed on alternate $-\frac{\pi}{3}$ lines starting on the V_{00} line and moving towards the right (blue lines in figure 20). Let us take a potential in one regular line with position coordinates (m_f, m_i) with respect to the $-\frac{\pi}{3}$ and horizontal lines, respectively. Then, the spectrum will consist of two sets: one is that of the HO, while the other is a finite one produced by m_f SUSY transformations separated by a gap of $\alpha - 2m_i$:

$$\mathcal{E} = \{\alpha - 2(m_i + m_f - 1), \ldots, \alpha - 2m_i\} \cup \{2, 4, 6, \ldots\}. \tag{64}$$

(iii) On the right of the $-\frac{\pi}{3}$ border line, between two $-\frac{\pi}{3}$ lines of regular potentials there is one filled with singular potentials ($V_{02}, V_{06}, \ldots$). The number of singularities also increases as we go down these lines.

(iv) Looking at the left side from the border line all the potentials have singularities following a rather complex pattern.

[7] We restrict the values of D to the positive axis because $u_\alpha(x, -D) = -u_\alpha(-x, D)$.

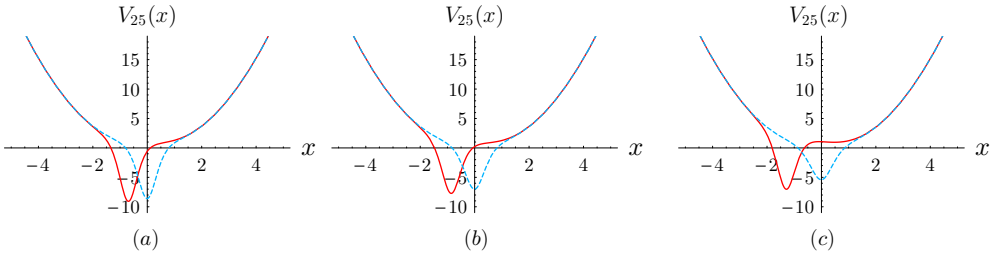

Figure 21. Confluent hierarchy potential $V_{25}(x)$ for different values of the eigenvalue α and the constant D: in continuous red $D = D_{\text{lim}} + 0.1$ and dashed blue $D = 100D_{\text{lim}}$. (a) $\alpha = 0.2$; (b) $\alpha = 1$; and (c) $\alpha = 1.8$.

(v) The effect of the arbitrary constant D is to modify the symmetry of the potential moving the minima and maxima. As the eigenvalue α becomes near 2 the shape becomes sharper.
(vi) The regular potentials for the values of D in case (ii) are placed on $-\frac{\pi}{3}$ lines containing $V_{02}, V_{06}, \ldots$.

As far as P_{IV} solutions are concerned, the only regular solutions are associated with arrows connecting regular potentials and those within cycles on the top horizontal line, also drawn in blue (figure 20).

All P_{IV} parameters included in this hierarchy can be obtained using equation (33) and taking into account that any cycle, up to an equivalence, has factorization eigenvalues $\{\alpha + 2n, \alpha + 2m, 0\}$ with $n, m \in \mathbb{Z}$ leading to two groups of parameters:

$$\begin{aligned} a &= 1 - \frac{\alpha}{2} + m - 2n; \qquad & b &= -\frac{1}{2}(\alpha + 2m)^2 \\ a &= \alpha - 1 + m + n; & b &= -2(m - n)^2. \end{aligned} \tag{65}$$

When the eigenfunction (62) has $\alpha = 1$ and constant $D = 2\frac{(A+B)\Gamma(5/4)}{(B-A)\Gamma(3/4)}$ the generated P_{IV} solutions coincide with those shown for the half-integer hierarchy in [9], where P_{IV} parameters take integer and half-integer values (65).

7.1. Example in the confluent hierarchy

As a simple example let us consider the potential V_{25} briefly. Its shape is shown in figure 21 for different values of the parameter D. It belongs to a cycle obtained after application of $\mathcal{T}_1\mathcal{R}$ four times to the starting cycle (figure 10). The third-order ladder operator of the Hamiltonian with this potential can be factorized as

$$\mathcal{L}_{V_{25}} = (\partial_x - (g_{14} + x))(\partial_x - x)(\partial_x - (g_{15} + x)) \tag{66}$$

where

$$g_{15}(x) = -2x + \frac{(\alpha - 4)g_{11}}{\alpha - 2 + 2xg_{11}} \tag{67}$$

$$g_{14}(x) = -\frac{(\alpha - 4)g_{11}}{\alpha - 2 + 2xg_{11}}, \tag{68}$$

and g_{11} is given in equation (63). As in the previous example (section 6.3), three eigenfunctions related to V_{25} outgoing arrows (see figure 20) are annihilated by the third-order creation operator (66) with eigenvalues $\alpha - 6$, $\alpha - 4$ and 0. The only one square-integrable is associated

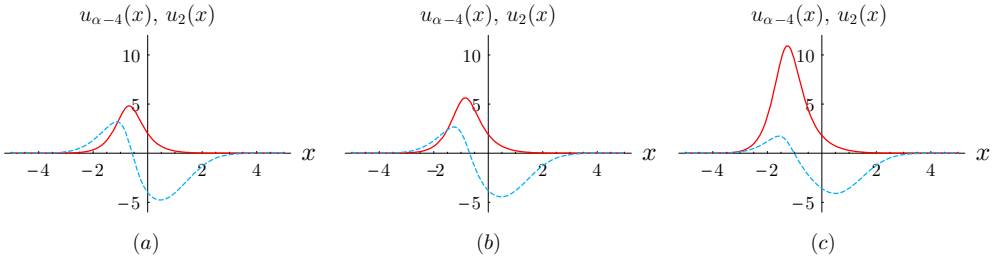

Figure 22. Two bottom eigenfunctions of $V_{25}(x)$ in the confluent hierarchy with eigenvalues: $\alpha-4$ in continuous red and two in dashed blue with constant value $D = D_{\text{lim}} + 0.1$. (*a*) $\alpha = 0.2$; (*b*) $\alpha = 1$; and (*c*) $\alpha = 1.8$.

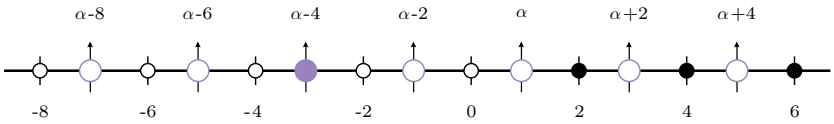

Figure 23. Diagram of V_{25} spectrum in the confluent hierarchy for $D \in (D_{\text{lim}}, \infty)$. The physical spectrum is represented by filled circles. The black and small circles constitute an infinite ladder while the purple is a finite one. The unfilled circles represent unphysical ladders of $\mathcal{L}^{\pm}$ operators.

with $\alpha-4$ and is the inverse of the function used to build the 1-SUSY relation between the HO in the horizontal line and V_{25}. The incoming arrows (see figure 20) give the eigenfunctions annihilated by the third-order lowering operator (adjoint of (66)) with eigenvalues $2, \alpha-2$ and again $\alpha-4$. As the eigenfunctions associated with the eigenvalues $\alpha-4$ and two are square-integrable (figure 22), the spectrum consists (figure 23) of two decoupled sets

$$\mathcal{E} = \{\alpha-4\} \cup \{2, 4, 6, \ldots\} \tag{69}$$

separated by a non-integer gap. This is in agreement with (64) taking $m_f = 1$ and $m_i = 2$. Note that the $\alpha-4$ eigenfunction is annihilated by both (lowering and raising) third-order operators because it is a one element set. Therefore, $\mathcal{L}_{V_{25}}$ join functions with eigenvalue $\alpha+2n$ on one side and $2m$ on the other. The special case $D = D_{\text{lim}}$ has the peculiarity of being regular and shares the same spectrum of HO, i.e., the eigenfunction associated with $\alpha-4$ is no longer square-integrable because on one side converges but on the other diverges having non-vanishing points.

8. The rotational hierarchy

This hierarchy corresponds to the unique rotational invariant point in the eigenvalue space (figure 9) and it is also related to a harmonic oscillator potential that we take as $V(x) = \frac{x^2}{9} + \frac{5}{3}$. This rescaling is made in order to have a standard shift of 2 units for the third-order ladder operator (15). The ground-level energy is now placed at $E_0 = 2$ and the gap between adjacent energy levels is $\frac{2}{3}$. Note the difference with respect to the other hierarchies where the steps of the HO spectrum and the third-order DLO coincide.

The starting cycle is obtained by applying the same first-order HO ladder operator three times, therefore all the potentials involved are equal except for the $\frac{2}{3}$ shifts, and the three P_{IV} solutions associated with this cycle are also the same (figure 24). Then, acting on this cycle we generate a hierarchy (figure 8) supporting the rotational symmetry with three equivalent

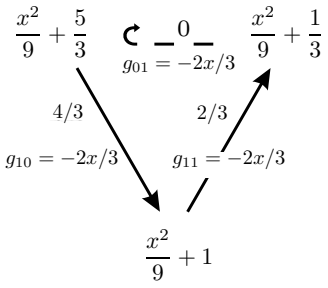

Figure 24. Starting cycle for rotational hierarchy.

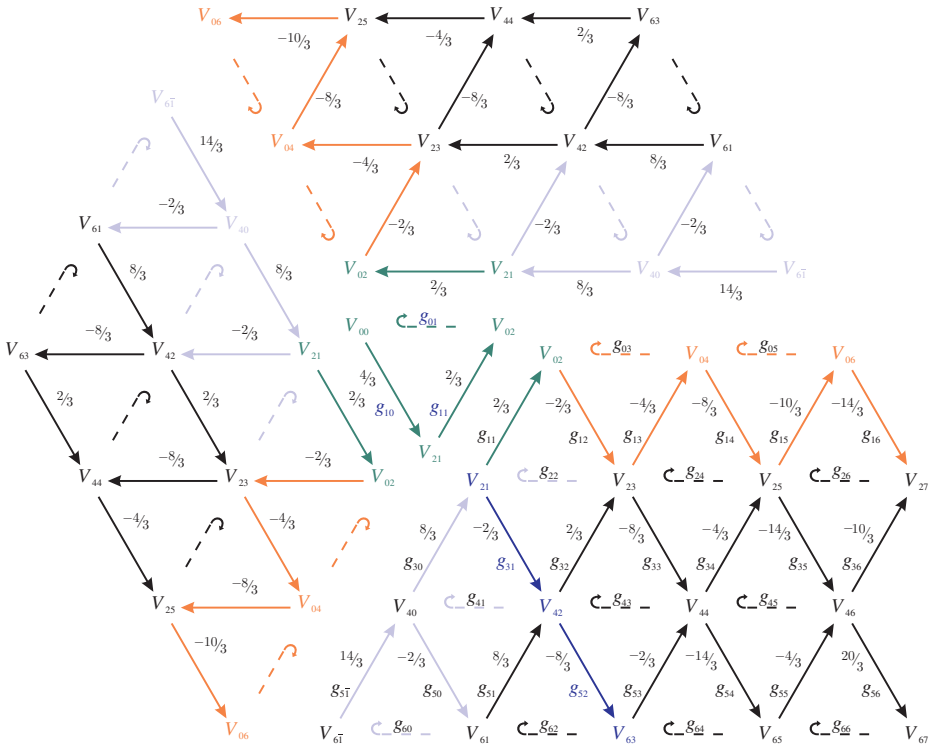

Figure 25. General scheme for rotational hierarchy.

regions transformed by global $\frac{2\pi}{3}$ rotations around the centre of the starting cycle as shown in figure 25.

Since the initial P_{IV} solutions are polynomial all the solutions obtained from them in the rotational hierarchy will be rational. Now, let us see how the regular and singular potentials are distributed as well as their spectrum properties in this hierarchy. We will fix our attention just in the bottom right sector.

The most interesting fact is that taking as usual the $-\frac{\pi}{3}$ lines as references to analyse the properties of this hierarchy, it is only found one of these lines filled with regular potentials: that starting with $V_{21}=\frac{x2}{9}+1$ and coloured in blue in figure 25. This is a quite different

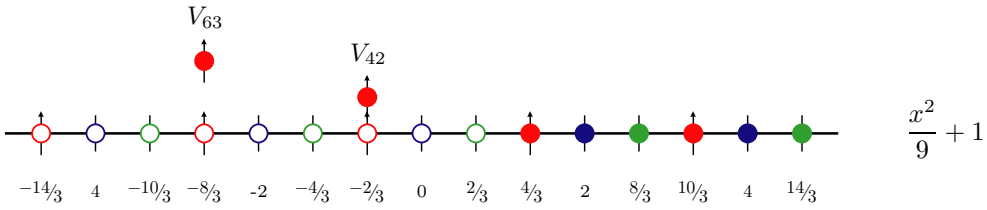

Figure 26. The bottom line represents the spectrum of the starting HO V_{21}. The physical energies are grouped into three infinite sets: green, blue and red, starting from the right. On the second line one added energy level shows the spectrum for first 1-SUSY regular potential V_{42} and, on the upper line one more level is added for V_{63}.

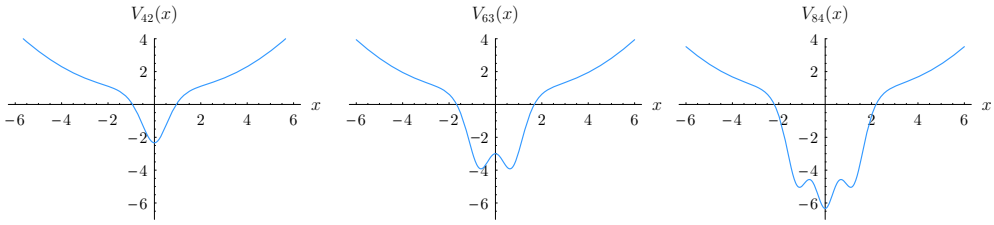

Figure 27. First regular potentials on the $-\frac{\pi}{3}$ line of V_{21}.

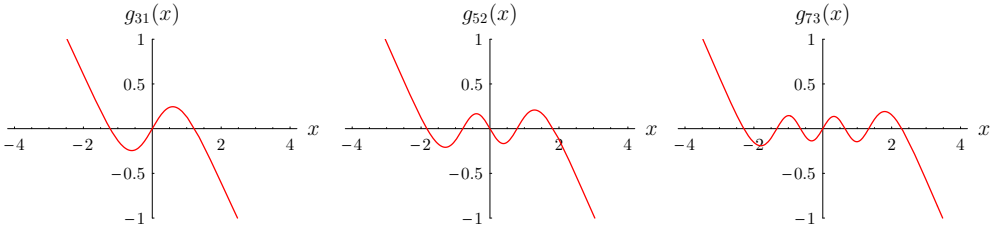

Figure 28. Regular P_{IV} solutions along the regular $-\frac{\pi}{3}$ line starting on g_{31}.

situation from that of the previous hierarchies but it is not difficult to understand it by means of SUSY transformations.

The spectrum of the starting HO is shown in figure 26 where the energy levels are grouped into three infinite disconnected sets because the ladder operator $\mathcal{L}$ connects levels separated steps of 2-units, while the shift of the first-order HO ladder operators $a^{\pm}$ is $\frac{2}{3}$. The Hamiltonians of the hierarchy are obtained by SUSY transformations from the initial HO, therefore regular ones have a spectrum differing at most in a finite set of points.

Since $\mathcal{L}$ is a third-order DLO annihilates just three eigenfunctions where there is a change of character from square-integrable to non-integrable functions, so new levels cannot be placed anywhere. It can be shown, applying the property of section 3.1, that the only way to enlarge this spectrum is by adding a set of new points starting from $-2/3$ downwards in 2-unit steps. The corresponding Hamiltonians fill the only regular blue $-\frac{\pi}{3}$ line in figure 27.

P_{IV} solutions have similar properties: regular solutions (figure 25) are also related to the V_{21} $-\frac{\pi}{3}$ line (blue in figure 25). The other solutions have singularities increasing their number as we move down along $-\frac{\pi}{3}$ direction. It is observed that the number of singularities

is invariant for P_{IV} solutions associated to $-\frac{\pi}{3}$ lines that are placed an even number of lines from the regular one ($g_{14}, g_{18}, \ldots$ and $g_{7\bar{1}}, g_{11\bar{3}}, \ldots$). The asymptotical behaviour is the same for all solutions i.e. $-2x/3$.

In the rotational hierarchy any P_{IV} solution can be related to a cycle with factorization eigenvalues written as $\left\{\frac{4}{3}+2n, \frac{2}{3}+2m, 0\right\}$ given general P_{IV} parameters (33):

$$a = m - 2n; \qquad b = -\tfrac{2}{9}(1+3m)^2. \tag{70}$$

9. Conclusions

In this work, we have designed a practical and useful geometric representation of the cycles describing the hierarchies of Hamiltonians with the third-order DLO. Each cycle can be considered at three different levels where the elements are: Hamiltonians (H_1, H_2, H_3), P_{IV} solutions (g_1, g_2, g_3) or factorization eigenvalues ($\alpha_1, \alpha_2, \alpha_3$) associated with the 1-SUSY transformations. As it is well known, the consistency of each cycle in order to obtain the third-order DLO is expressed as a P_{IV} equation.

We have defined operations on the cycles which correspond to properties of the DLO considered as a 3-SUSY transformation. These operations are easily represented in our geometrical diagrams giving rise to a lattice describing the Hamiltonian hierarchy.

Three types of cycles generate three kinds of hierarchies, each of them with particular symmetries. A realization of each of these hierarchy types have been given starting with the Hamiltonian of the harmonic oscillator. In such realizations we have investigated the spectrum of the new Hamiltonians involved, regularity properties of P_{IV} solutions, as well as the relations through SUSY transformations. These properties are regularly displayed in the geometric representation in an easy way, enabling us to know characteristics of potentials and P_{IV} solutions without knowing their specific expression. Some examples have been worked out to illustrate these properties. We have also shown the relation of the spectrum of the Hamiltonians in each hierarchy with the different kinds of representations of the $\mathcal{L}^{\pm}$ algebra.

Acknowledgments

This work has been partially supported by SpanishMEC (ProjectMTM2005- 09183), by Spanish JCyL (Excellence Project VA013C05) and by a JCyL Research Grant. We are grateful to L M Nieto, J M Cervero and M V Ioffe for useful discussions.

References

[1] Carballo J M, Fernández D J, Negro J and Nieto L M 2004 Polynomial Heisenberg algebras *J. Phys. A: Math. Gen.* **37** 10349–62

[2] Fernandez D J, Negro J and Nieto L M 2004 Elementary systems with partial finite ladder spectra *Phys. Lett.* A **324** 139–44

[3] Sukumar C V 1985 Supersymmetric quantum-mechanics of one-dimensional systems *J. Phys. A: Math. Gen.* **18** 2917–36

[4] Bagrov V G and Samsonov B F 1997 Darboux transformation of the Schrödinger equation *Phys. Part. Nucl.* **28** 374–97

[5] Adler V E 1994 Nonlinear chains and Painlevé equations *Phys.* D **73** 335–51

[6] Andrianov A A, Cannata F, Ioffe M V and Nishnianidze D N 2000 Systems with higher-order shape invariance: spectral and algebraic properties *Phys. Lett.* A **266** 341–9

[7] Ioffe M V and Nishnianidze D N 2004 SUSY intertwining relations of third order in derivatives *Phys. Lett.* A **327** 425–32

[8] Veselov A P and Shabat A B 1993 Dressing chains and the spectral theory of the Schrödinger operator *Funct. Anal. Appl.* **27** 81–96
[9] Bassom A P, Clarkson P A and Hicks A C 1995 Bäcklund transformation and solution hierarchies for the fourth Painlevé equation *Stud. Appl. Math.* **95** 1–71
[10] Clarkson P A 2003 The fourth Painlevé equation and associated special polynomials *J. Math. Phys.* **44** 5350–74
[11] Sen A, Hone A N W and Clarkson P A 2005 Darboux transformations and the symmetric fourth Painlevé equation *J. Phys. A: Math. Gen.* **38** 9751–64
[12] Cooper F, Khare A and Sukhatme U 1995 Supersymmetry and quantum-mechanics *Phys. Rep. Rev. Sec. Phys. Lett.* **251** 268–385
[13] Sukumar C V 1985 Supersymmetry, factorization of the Schrödinger-equation and a Hamiltonian hierarchy *J. Phys. A: Math. Gen.* **18** L57–61
[14] Sukumar C V 1986 Supersymmetry, potentials with bound-states at arbitrary energies and multisoliton configurations *J. Phys. A: Math. Gen.* **19** 2297–316
[15] Junker G 1996 Supersymmetric methods in quantum and statistical physics *Texts and Monographs in Physics* (Berlin: Springer)
[16] Samsonov B F 1999 New possibilities for supersymmetry breakdown in quantum mechanics and second-order irreducible Darboux transformations *Phys. Lett.* A **263** 274–80
[17] Rosas-Ortiz O and Munoz R 2003 Non-Hermitian SUSY hydrogen-like Hamiltonians with real spectra *J. Phys. A: Math. Gen.* **36** 8497–506
[18] Andrianov A A, Cannata F, Dedonder J-P and Ioffe M V 1995 2nd-order derivative supersymmetry, q-deformations and the scattering problem *Int. J. Mod. Phys.* A **10** 2683–702
[19] Mielnik B and Rosas-Ortiz O 2004 Factorization: little or great algorithm? *J. Phys. A: Math. Gen.* **37** 10007–35
[20] Bagrov V G and Samsonov B F 1995 Darboux transformation, factorization, and supersymmetry in one-dimensional quantum mechanics *Theor. Math. Phys.* **104** 1051–60
[21] Andrianov A A, Ioffe M V and Spiridonov V P 1993 Higher-derivative supersymmetry and the Witten index *Phys. Lett.* A **174** 273–9
[22] Fernandez D J and Hussin V 1999 Higher-order SUSY, linearized nonlinear Heisenberg algebras and coherent states *J. Phys. A: Math. Gen.* **32** 3603–19
[23] Fordy A P, Shabat A B and Veselov A P 1995 Factorization and Poisson correspondences *Theor. Math. Phys.* **105** 1369–86
[24] Fordy A P and Gibbons J 1980 Factorization of operators: I. Miura-transformations *J. Math. Phys.* **21** 2508–10
[25] Clarkson P A, Hone A N W and Joshi N 2003 Hierarchies of difference equations and Bäcklund transformations *J. Nonlinear Math. Phys.* **10** 13–26
[26] Okamoto K 1986 Studies on the Painlevé equations: III. Second and fourth Painlevé equations *Math. Ann.* **275** 221–55
[27] Humphreys J E 1990 Reflection groups and coxeter groups *Cambridge Studies in Advance Mathematics* vol 29 (Cambridge: Cambridge University Press)
[28] Junker G and Roy P 1998 Conditionally exactly solvable potentials: a supersymmetric construction method *Ann. Phys.* **270** 155–77
[29] Cooper F, Ginocchio J N and Khare A 1987 Relationship between supersymmetry and solvable potentials *Phys. Rev.* D **36** 2458–2473